Formulation of an eco-binder based on calcined sediment, ground granulated blast furnace slag, and waste paper fly ash

Zeinab MKAHAL[1,2], Walid MAHERZI[1,2], Mahfoud BENZERZOUR[1,2], Nor-edine ABRIAK[1,2]

[1] *IMT Nord Europe, Institut Mines-Télécom, Centre for Materials and Processes, Environnement, F-59000 Lille, France.*

[2] *Univ. Lille, Univ., ULR 4515 – LGCgE, Laboratoire de Génie Civil et géo-Environnement, F-59000 Lille, France.*

Abstract

The formulation of an eco-binder based on alternative materials only makes sense if its technical and environmental relevance has been evaluated. This study focuses on the effect of replacing up to 60% of Portland cement with calcined sediment, ground granulated blast furnace slag, and waste paper fly ash. The numerical analysis to choose the formulation was carried out by using commercial software (Design Expert) dedicated to experimental modeling designs. Water demand, setting time, volume expansion, compressive strengths, and heat of hydration (Langavant calorimetry) were performed to evaluate the effect of replacing cement with alternative materials on matrix properties. The results reveal that the proposed mixes meet the specifications of many hydraulic binders. Since the production of one ton of cement generates 780 kg of CO_2 (He *et al.*, 2019), replacing ordinary Portland cement with alternative materials reduces greenhouse gas emissions.

Keywords

Calcined sediment, ground granulated blast furnace slag, waste paper fly ash, and Eco-binder.

I. INTRODUCTION

The management of dredged sediments is based on technical, socio-economic, and environmental challenges and issues. This is why pre-treatment and treatment processes have been set up. These processes aim to improve specific properties or neutralize pollutants for recovery purposes.

The valorization of sediments in the cement industry has been studied for the elaboration of hydraulic binders in the raw material and more recently in the substitution of clinker (el Mahdi Safhi *et al.*, 2019). Generally, physical and thermal treatments were carried out before the addition of sediments to the cement matrix. Grinding (physical treatment) contributes to the improvement of their fineness, while the calcination (thermal treatment) activates some of their phases like calcite $CaCO_3$ but also the essential phases for the pozzolanic activity like the clays (kaolinite) (AMAR *et al.*, 2021). Similarly, calcination leads to the degradation of organic phases that affect the mechanical properties of the matrix.

This work is divided into two main parts. The first one focuses on sediment calcination, with a study to optimize calcination parameters in a static oven. This part is not presented in this article. However, the calcination of sediments SBF from the natural dewatering site of "La Hisse" was set for a duration of 1 h at a temperature of 850 °C (determined by thermogravimetric analysis) to ensure optimal pozzolanic reactivity and to avoid the risk of recrystallization.

The second part aims at optimizing formulations based on CEMI 42.5N, Calcinated sediments (SBF-C), Ground Granulated Blast-Furnace Slag (GGBS), and waste paper fly ash (WPFA).

II. METHODOLOGY

Fig. 1 describes the experimental approach followed in our study.

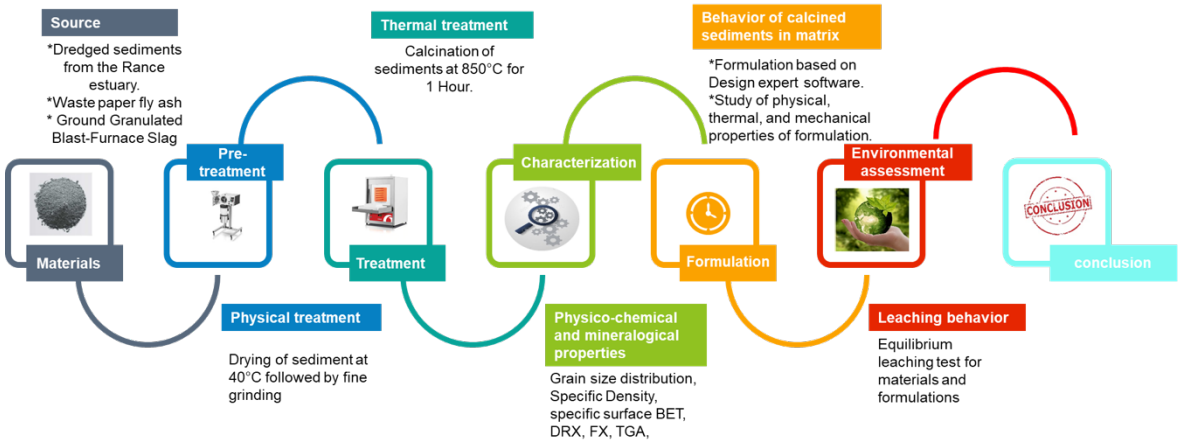

Fig. 1 Experimental approach adopted for the valorization of calcined dredged sediments in eco-binders.

III.CHARACTERIZATION OF THE MATERIALS

A. Grain size distribution

The granulometric analysis by laser technique is carried out on all the studied materials. The first observation that can be noted is the similarity of the granulometry of CEM and GGBS with D_{max} of 33µm and D_{50} around 9µm (Fig. 2). The physical treatment (grinding) of sediments allows for obtaining the finest material SBF-G with D_{max} of 33µm also and D_{50} of 6.7µm. Comparing the SBF-C with the SBF-G, it can be seen that calcination has changed the fineness as well as the shape of the particles (enlargement and swelling) with D_{max} of 230µm and D_{50} of 10.8µm. This allows us to deduce that the coarsest grains have undergone a sintering process by welding or swelling phenomena occurring under the effect of heat (BERNACHE-ASSOLLANT and BONNET, 2005). In addition, WPFA represents the coarsest material with a D_{max} of 370 µm and a D_{50} of 111 µm.

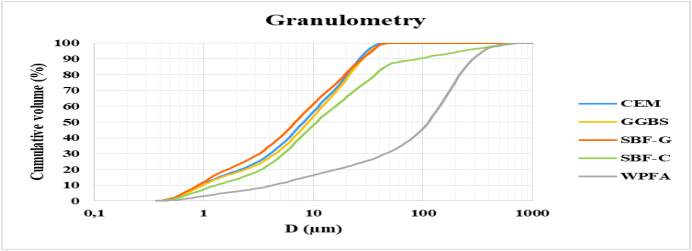

Fig. 2 Grain size distribution of CEMI 42.5N, SBF-G, SBF-C, GGBS, and WPFA.

B. Specific Density and BET-specific surface area

The Specific density was measured according to NF EN 1097-7, using a helium pycnometer type AccuPyc 1330 (Micromeritics). The BET-specific surface area test was carried out according to the standard NF EN ISO18757, 2006, using an apparatus of model Micromeritics Autopore IV 9505.

These results show that the alternative materials have lower densities than cement and that SBF-G represents the smallest value among them (2.65 g/cm^3) (Table 1). It is important to note that calcination improved the density of the sediment, which may be the result of an intensive densification process and the elimination of OM (AMAR, 2017).

BET-specific surface area makes it possible to evaluate the fineness of the additions and brings an indication of the reactivity (pozzolanicity). The results show significant changes between the raw and calcined sediments (Table 1). Calcination reduced the BET-specific surface area from 141,643 cm^2/g for SBF-G to 24,086 cm^2/g for SBF-C, probably by sintering. It should also be noted that SBF-C has the same fineness as WPFA, but is superior to cement and GGBS.

The results confirm that the calcination influences the fineness and the density of sediments by the sintering effect (or densification) and the elimination of the organic and volatile constituents.

Table 1. Determination of the Specific density (g/cm3) and the BET-specific surface of the studied materials.

	CEM	SBF-G	SBF-C	WPFA	GGBS
Specific Density (g/cm^3)	3.15	2.65	2.84	2.99	2.96
BET Surface area (cm^2/g)	13,260	141,643	24,086	24,285	13,979

C. Mineralogical analysis

Mineralogical characterization is performed primarily by X-ray diffraction (XRD) analysis using a Bruker D8 Advance diffractometer equipped with a cobalt anode ($\lambda K\alpha 1$ = 1.74 Å).

The XRD spectra of the CEM (Fig. 3 (a)) show the presence of peaks that corresponds to the main phases of Portland cement (Alite C_3S, Anhydrite $CaSO_4$, Aluminate C_3A, and Ferrite C_4AF).

The minerals present in the WPFA are Gehlenite, Calcite, Quicklime, Portlandite, Quartz, α'-C_2S (Ca_2SiO_4), Mayenite, and Anhydrite (Fig. 3 (b)). Indeed, the potentially reactive minerals (lime, Mayenite, and α'-C_2S) give the WPFA interesting hydraulic properties (MOZAFFARI *et al.*, 2009).

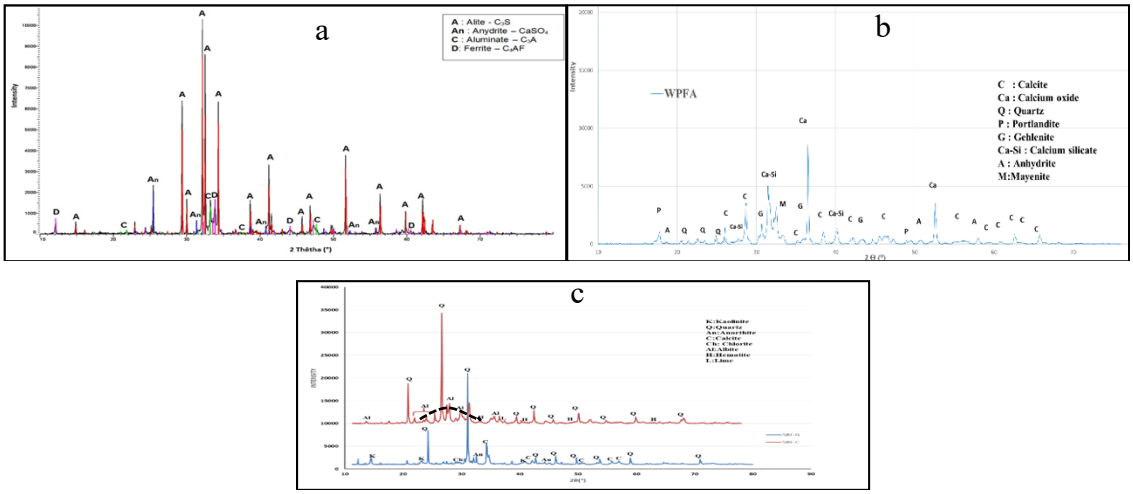

Fig. 3 XRD analysis on CEM (a), WPFA (b), and SBF-G and SBF-C (c).

The interpretation of the diffractogram of SBF-G and SBF-C (Fig. 3 (c)) shows that the SBF-G is composed of Quartz, Calcite, and Aluminosilicate (Kaolinite, Chlorite, and Anorthite). These analyses revealed significant mineralogical changes. The heat probably initiated some physicochemical processes. XRD shows a disappearance in peak phases such as Calcite due to the decarbonation phase followed by the appearance of free Lime in SBF-C. Similarly, clay phases such as Kaolinite could be transformed into Metakaolin by a dehydroxylation process. Finally, the bulge observed (amorphization curve) corresponds to the amorphous phases that appeared to be non-existent in SBF-G. The characteristic peaks of Hematite and Albite were detected in the calcined sediments.

However, the diffractogram of the blast furnace slag is not presented. It reveals the presence of a perfectly vitrified material (Houze, 2014).

D. Chemical composition

CEM, GGBS and WPFA (Table 2) shows a typical chemical composition of materials already studied in the literature (Siddique and Bennacer, 2012), (Ehsani *et al.*, 2023), (MOZAFFARI *et al.*, 2009). The basicity index of the GGBS is about 1.07 (>0.9), which may reflect a high hydraulic capacity. The high CaO content brings the composition of WPFA close to the typical composition of Portland cement with a basicity index of 2.3.

After calcination of SBF, the concentration of silicon oxide is higher. This increase is mainly due to the removal of organic compounds and carbonates. According to (ASTM C618 -19, 2008) which is used to evaluate the level of pozzolanicity of materials, the sum of Al_2O_3 + SiO_2 + Fe_2O_3 reaches 61.8% for SBF-G and 67.4% for SBF-C. This value is close to what is required in the standard (>70%), especially for SBF-C.

Table 2. Oxides (%) present in the materials CEM, SBF-G, SBF-C, GGBS, and WPFA.

	SiO_2	Al_2O_3	MgO	Fe_2O_3	CaO	Na_2O	K_2O	P_2O_5	SO_3	TiO_2	MnO	Cl	ZnO
CEMI	17.38	4.87	0.85	2.84	59.00	0.26	1.00	-	4.35	0.39	-	-	-
WPFA	14.49	10.72	1.68	1.01	56.80	0.68	0.72	0.43	2.29	0.76	-	1.05	0.21
GGBS	32.94	10.58	6.49	0.44	40.25	0.32	0.51	-	1.64	0.78	0.22	-	-
SBF-G	42.73	13.79	1.96	5.30	15.29	1.00	2.49	0.31	1.37	0.64	-	0.15	-
SBF-C	46.33	14.95	2.20	6.12	17.32	1.06	2.76	0.35	2.26	0.69	-	0.19	-

IV. .BEHAVIOR OF CALCINATED SEDIMENTS IN THE CEMENTITIOUS MATRICES

A. Experimental design

Several researchers have revealed the importance of using the design of experiments (DOE) in civil engineering, especially for the optimization of cementitious mixtures (Matos *et al.*, 2018)(Imanzadeh *et al.*, 2018). In our study, DOE is used to quantify the influence of each component of the mixture on the mortar's unconfined compressive strength. The main characteristic of a random mixture is that the sum of CEM, SBF-C, WPFA and GGBS (taken in mass proportion) must equal 1 (100%).

Moreover, the optimal mixture design method specifies the range of the variation of different components (low and high constraints). These limits must be between the values of 0 and 1 (Table

3). The numerical analysis was carried out by using commercial software (Design Expert) dedicated to experimental modeling designs. The dedicated software gives the mix proportions of a total of 15 points for modeling. **Table 4** presents the determined arrangements of the 15 runs.

Table 3. Limits of the mixture components.

Component mass	CEM	SBF-C	WPFA	GGBS
Lower constraints	0.4	0	0	0
Higher constraints	1	0.6	0.6	0.6

B. Preparation of specimens

The method of mixing, molding, and curing the specimens is based on the NF EN 196-1 standard. **Table 4** summarizes the compressive strengths obtained at 56 days for the 15 proposed mixes.

Table 4. Proportions of the components of the 15 mixtures proposed for modeling and their corresponding Rc.

	F1	F2	F3	F4	F5	F6 (R)	F7	F8	F9	F10	F11	F12	F13	F14	F15	D1	D2	D3
SBF-C	0	30	15	30	0	0	30	7.5	7.5	0	60	0	0	37.5	7.5	13.5	18	24
WPFA	0	0	15	0	60	0	30	37.5	7.5	30	0	0	30	7.5	7.5	0.7	1.4	1
GGBS	60	30	15	0	0	0	0	7.5	37.5	30	0	30	0	7.5	7.5	45.8	40.6	35
CEM	40	40	55	70	40	100	40	47.5	47.5	40	40	70	70	47.5	77.5	40	40	40
Rc 56 days (MPa)	44.4 ± 2.5	37.2 ± 1.9	28.2 ± 0.9	34.3 ± 2.3	10.3 ± 0.1	51.6 ± 1.2	16.8 ± 0.2	18.9 ± 0.9	36.7 ± 3.5	24.6 ± 0.2	20.8 ± 0.5	52.4 ± 1.1	25.5 ± 1.9	31.2 ± 4.2	42.3 ± 4.7	36.4 ± 2.4	31.9 ± 0.4	28.7 ± 1.2

C. Results and Discussion

1. Validation of the model

The compressive strength results at 56 days for the 15 proposed mixes were modeled using the linear Scheffe model. The linear model was selected instead of another model because it represents the most suitable model based on the values of p-value, adjusted R^2, and predicted R^2, conforming to guidelines. The p-value was statistically significant and lower than 0.05 while the adjusted and predicted R^2 were very close to 1 and their difference was lower than 0.2.

Fig. 4 illustrates a response surface (2D and 3D) with different color shades from dark blue (i.e., lower resistance) to red (i.e., higher resistance). The selected regression model equation relating the compressive strength (Rc) of the mixture to the four variables CEM, SBF-C, WPFA, and GGBS is detailed in eq.1.

$$Rc\ (MPa) = +1.83*SBF\text{-}C - 18.17*\ WPFA + 38.87*\ GGBS + 51.41*\ CEM. \quad (eq.1)$$

From the model, 3 formulations (D1, D2, and D3) were chosen (Table 4). The first criterion taken into account when selecting the three mixes was to minimize the proportion of cement to 40% and to meet the specifications for normal hardening hydraulic road binders (HRB), especially N4 (Rc (56 days ≥ 32,5 MPa). To validate the selected regression model, the compressive strength of the three chosen mixes was tested after 56 days of curing. Table 5 shows that only the compressive strength of the D1 mixture, which was determined experimentally, was well within the 95% confidence interval (CI). For D2 and D3, the experimentally obtained resistances do not respect

the 95% confidence interval. To confirm the suitability of the selected model for formulations with low percentages of SBFC-C, it is necessary to subsequently formulate other formulations containing less than 13.5% SBFC-C.

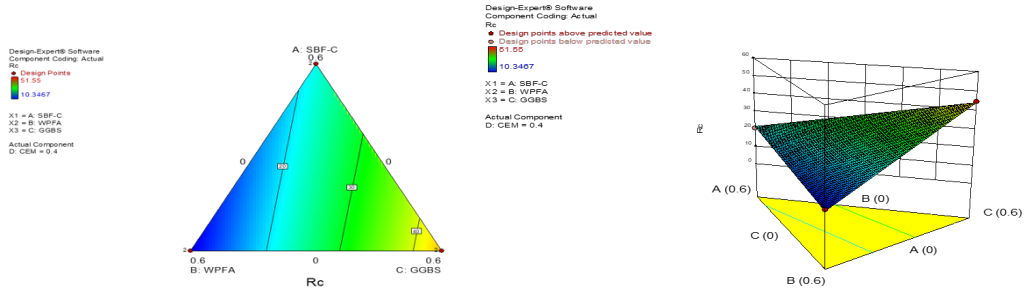

Fig. 4. 2D (left) and 3D (right) response surfaces.

Table 5. Predicted and experimental UCS after 56 days of curing.

	Model Predicted Rc (MPa)	Experimental Rc (MPa)	95% CI (MPa)
D1	38.48%	36.4 ± 2.4%	[35.89-41.07]
D2	36.42%	31.9 ± 0.4%	[34.03-38.80]
D3	34.43%	28.7 ± 1.2%	[32.16-36.68]

2. Evolution of physical properties

Water demand

WPFA and SBF-C have a higher water demand than the other materials with W/C of 0.87 and 0.47 respectively. GGBS and CEM represent the same water demand (W/C=0.34). The W/C of R, D1, D2, and D3 were 0.35, 0.37, 0.38, and 0.40 respectively. Thus, the addition of WPFA and SBF-C increases water demand when used as a partial replacement for cement, which is not the case for GGBS. This is mainly due to their high specific surface (WPFA and SBF-C) and their mineralogical phases (especially WPFA). However, R1 has the lowest W/C ratio. The increase in the W/C ratio in the selected formulations is mainly attributed to the increase in sediment content (ZERAOUI, 2021)(AMAR, 2017)(el Mahdi Safhi *et al.*, 2019).

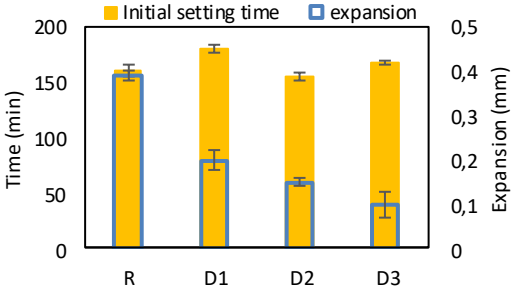

Fig. 5 Initial setting time, expansion, and W/C ratio for the used materials and chosen formulations.

Initial setting time

Comparing the different formulations with the control, it can be seen that D1 and D3 represent a delay in the initial setting time of 20 and 7 min respectively, which is not the case for D2 with 5 min of acceleration (Fig. 5). Note that D2 contains relatively the highest percentage of WPFA (1.4%) compared to D1 and D3. Therefore, according to these results, we can say that the addition of sediments in the cementitious matrix causes a delay in the initial setting time which can be attributed to the additional water content added to compensate for the water absorbed by the fine sediments (Xu *et al.*, 2022). According to the literature, WPFA is known for its fast setting due to its fineness and the presence of free lime in great quantity (HU, GE and WANG, 2014). From these results, it is important to note that despite the low percentage of WPFA in the formulations they have more influence on the setting time than the sediments.

It can be seen that the 3 formulations meet the setting time requirements which must be at least 90 minutes for rapid hardening hydraulic road binder (HRB-R) classes (E2, E3, and E4) and at least 150 minutes for normal hardening hydraulic road binder (HRB-N).

Stability

The stability test ensures that the binder produced does not contain substances that could cause dangerous expansion over time. The constituents of the binder which are responsible for an expansion are gypsum and free lime. According to NF EN 13282-1 and NF EN 13282-2, the expansion must be ≤ 10 mm and ≤ 30 mm for rapid and normal hardening HRB, respectively.

According to Fig. 5, the reference has the highest expansion value (0.39 mm) while remaining far from the limit suitable for road hydraulic binders (<10 mm). For formulations, the expansion decreases with the increase of the incorporation rate of SBF-C. This result is confirmed by the low sulfate contents found in SBF-C (2.26%) compared to the higher values in CEM I (4.35%) (Table 2). Therefore, it can be stated the partial replacement of CEMI by SBF-C, WPFA, and GGBS contributes to improving the stability of formulations which can be used as HRB-R and HRB-N.

Influence of the addition of calcinated sediment and waste paper fly ash on the hydration kinetics (Langavant Calorimetry)

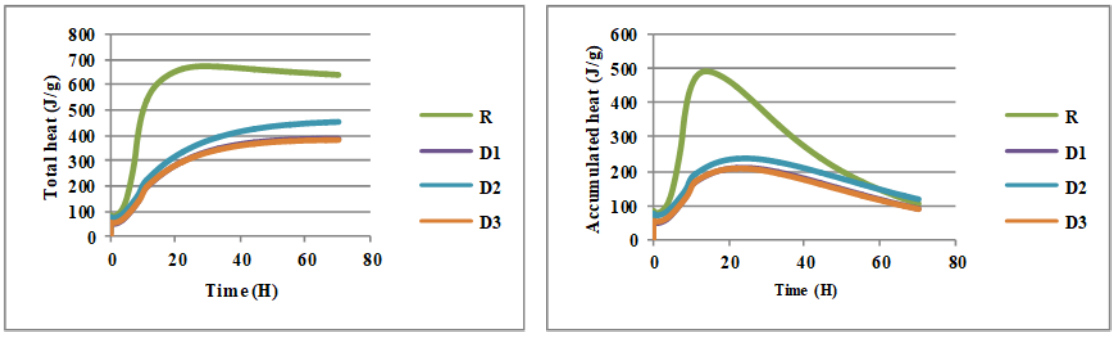

Fig. 6 Total (left) and Accumulated (right) hydration heat measured for reference, D1, D2, and D3 mortar.

Ordinary cement is characterized by rapid hydration that reaches 95% of its final value at 14.8 hours of age (Fig. 6, left). This has positive consequences on the stiffness and negative consequences on the microstructure which will be vulnerable to early cracking if no curing measures are used.

All three formulations represent lower heat release than cement alone due to the dilution effect, delayed pozzolanic reaction of calcined sediments, and latent hydraulicity of GGBS (AMAR, 2017). In addition, the formulations reach 95% of their final value after 47.63 hours for D2 and 41.93 hours for D1 and D3.

However, the total heat released by D2 is higher than those of D1 and D3 which represent superimposed curves. This may be attributed to the relatively higher WPFA content in D2 (presence of hydraulic phases such as lime, mayenite, and α'-C2S (Ca_2SiO_4)).

Indeed, the peak obtained in the curves of the accumulated heat of hydration corresponds to the phase following the "End of setting" (Fig. 6, right). This results in a maximum release of heat, generated by all the reactions of dissolution, precipitation, and formation of the various hydrates (HU, GE and WANG, 2014). The reference has a higher maximum heat value than the formulations, which is reached at 28h. It is important to note that for all three formulations (D1, D2, and D3) the maximum heat accumulation is reached almost at the same time (about 48h). However, D2 reveals a higher maximum value than D1 and D3 (Fig. 6, right).

3. *Evolution* of mechanical properties (Compressive strength)

Fig. 7 summarizes the activity index which is generally determined to evaluate the contribution of the additives to the mechanical strength. It is the ratio between the mechanical strength of a standard mortar (100% cement) and the mechanical strength of a mortar containing a mass percentage of the additive to be tested instead of cement. In this study, this ratio was determined for the three formulations at different times to understand the evolution of the mechanical strength in time.

From a global point of view, no formulation was able to reach the mechanical strength of the control mortars. It is important to note that the activity index increases in all formulations up to 56 days to 71%, 62%, and 56% for D1, D2, and D3 respectively.

According to **Table 4**, the presence of WPFA as an admixture in the cementitious matrix is responsible for the large loss of strength in the formulations (especially F3, F5, F7, F8, F10, and F13). On the other hand, the presence of GGBS in the formulations contributes to the increase in compressive strength. This is visible in formulation F12 where the replacement of cement by 30% GGBS gives a higher strength than the reference mortar (F6). Formulations (F2, F9, F11, F14, and F15) containing both sediment and slag with low WPFA percentages (between 0 and 7.5%) contribute to the strength development because the loss of strength is less than the cement replacement rate. For example, the activity index of F9 (with 37.5% GGBS) and F14 (with 37.5% SBF-C), which contain the same rate of cement (47.5%) and WPFA (7.5%), was 71% and 60% respectively. Hence, the gain in resistance for F9 and F14 are 18.6 and 7.9% respectively.

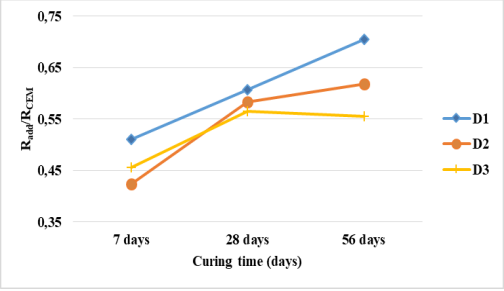

Fig. 7 Evolution of the ratio between the compressive strength of WPFA-C and CEMI as a function of the curing time.

After 56 days of curing, the compressive strengths of D1, D2, and D3 were 36.3, 31.8, and 28.66 MPa, respectively. Comparing the strengths obtained at 56 days with the HRB specifications D1 can be used as a Class N4 HRB while D2 and D3 are considered Class N3 HRBs.

V. CONCLUSION

The objective of this study was the formulation of eco-binders based on alternative materials. The additives used were calcined sediments (SBF-C), ground granulated blast furnace slag (GGBS), and waste paper fly ash (WPFA). A design of experiments approach was used to determine the optimal proportions of each compound was used. The goal was to replace 60% of the cement with the additions. The mortars were manufactured and then tested in compression at 56 days. The exploitation of the results allowed us to define a mathematical model. This model was verified by the formulation of 3 new mixtures. The results show that the predictions made by the model are validated only for low SBFC-C contents (13.5%).

The effect of the incorporation of alternative materials and more particularly of calcined sediments in a cementitious matrix on the characteristics of mortars in the fresh and hardened state was studied on the three selected formulations. Indeed, the addition of sediments in the cementitious matrix leads to an increase in the W/C ratio, a delay in the initial setting time, and an improvement in the stability.

Moreover, the heat of hydration control test by the semi-adiabatic method showed that the Eco-binders allows to obtain lower heats of hydration than Portland cement alone, which is due to the dilution effect, the delayed pozzolanic reaction of the calcined sediments, and the latent hydraulicity of GGBS.

The results showed that, although the mechanical performances of the formulations based on alternative materials are still lower than those of the control (100% CEM), the strengths obtained at 56 days allow the use of eco-binders as hydraulic road binders. It is interesting to note that the sediments contribute like GGBS but to a lesser extent to the strength development.

VI. REFERENCE

AMAR, M. *et al.* (2021) 'From dredged sediment to supplementary cementitious material: characterization, treatment, and reuse', *International Journal of Sediment Research*. Elsevier Ltd, 36(1), pp. 92–109. doi: 10.1016/j.ijsrc.2020.06.002.

AMAR, M. A. A. (2017) *Traitement des sédiment de dragagge pour une valorisation dans les matrice cimentaires*. IMT - Institut Mines Télécom - Lille Douai. Available at: https://ori-nuxeo.univ-lille1.fr/nuxeo/site/esupversions/0f4f5ddf-c741-4135-87b3-0ef6d9be0906.

ASTM C618 -19 (2008) *Standard Specification for Coal Fly Ash and Raw or Calcined Natural Pozzolan for Use in Concrete, West Conshohocken, PA: Annual Book of ASTM Standards ASTM International, .*

BERNACHE-ASSOLLANT, D. and BONNET, J.-P. (2005) *Frittage : aspects physico-chimiques - Partie 1 : frittage en phase solide*, *Fabrication additive – Impression 3D*. doi: 10.51257/a-v1-af6620.

Ehsani, A. *et al.* (2023) 'The positive effects of power ultrasound on Portland cement pastes and mortars ; a study of chemical shrinkage and mechanical performance', *Cement and Concrete Composites*. Elsevier Ltd, 137(January), p. 104935. doi: 10.1016/j.cemconcomp.2023.104935.

He, Z. *et al.* (2019) 'Comparison of CO 2 emissions from OPC and recycled cement production', *Construction and Building Materials*. Elsevier Ltd, 211, pp. 965–973. doi:

10.1016/j.conbuildmat.2019.03.289.

Houze, C. (2014) *Étude de la valorisation des laitiers de l ' industrie sidérurgique et de production des alliages silico manganèse Clément Houze To cite this version : HAL Id : tel-00957552 Etude de la valorisation des laitiers de l ' industri e sidérurgique et de produc*.

HU, J., GE, Z. and WANG, K. (2014) 'Influence of cement fineness and water-to-cement ratio on mortar early-age heat of hydration and set times', *Construction and Building Materials*. Elsevier Ltd, 50, pp. 657–663. doi: 10.1016/j.conbuildmat.2013.10.011.

Imanzadeh, S. *et al.* (2018) 'Formulating and optimizing the compressive strength of a raw earth concrete by mixture design', *Construction and Building Materials*. Elsevier Ltd, 163, pp. 149–159. doi: 10.1016/j.conbuildmat.2017.12.088.

el Mahdi Safhi, A. *et al.* (2019) 'Feasibility of using marine sediments in SCC pastes as supplementary cementitious materials', *Powder Technology*. Elsevier B.V., 344, pp. 730–740. doi: 10.1016/j.powtec.2018.12.060.

Matos, A. M. *et al.* (2018) 'Design of self-compacting high-performance concrete: Study of mortar phase', *Construction and Building Materials*, 167, pp. 617–630. doi: 10.1016/j.conbuildmat.2018.02.053.

MOZAFFARI, E. *et al.* (2009) 'An investigation into the strength development of Wastepaper Sludge Ash blended with Ground Granulated Blastfurnace Slag', *Cement and Concrete Research*. Elsevier B.V., 39(10), pp. 942–949. doi: 10.1016/j.cemconres.2009.07.001.

Siddique, R. and Bennacer, R. (2012) 'Use of iron and steel industry by-product (GGBS) in cement paste and mortar', *Resources, Conservation and Recycling*. Elsevier B.V., 69, pp. 29–34. doi: 10.1016/j.resconrec.2012.09.002.

Xu, W. *et al.* (2022) 'Improvement in water resistance of magnesium oxychloride cement via incorporation of dredged sediment', *Journal of Cleaner Production*. Elsevier Ltd, 356(December 2021), p. 131830. doi: 10.1016/j.jclepro.2022.131830.

ZERAOUI, A. (2021) *Approche opérationnelle pour une gestion durable des sédiments de dragage dans des filières de génie civil : mise en place d'un outil d'aide à la décision*. IMT Lille Douai.